Unsteady flow of a thixotropic fluid in a slowly varying pipe

Andrew I. Croudace, David Pritchard,[a] and Stephen K. Wilson
Department of Mathematics and Statistics, University of Strathclyde, 26 Richmond St., Glasgow G1 1XH, Scotland, United Kingdom

(Received 1 April 2017; accepted 1 August 2017; published online 21 August 2017)

We analyse the unsteady axisymmetric flow of a thixotropic or antithixotropic fluid in a slowly varying cylindrical pipe. We derive general perturbation solutions in regimes of small Deborah numbers, in which thixotropic or antithixotropic effects enter as perturbations to generalised Newtonian flow. We present results for the viscous Moore–Mewis–Wagner model and the viscoplastic Houška model, and we use these results to elucidate what can be predicted in general about the behaviour of thixotropic and antithixotropic fluids in lubrication flow. The range of behaviour we identify casts doubt on the efficacy of model reduction approaches that postulate a generic cross-pipe flow structure. [http://dx.doi.org/10.1063/1.4998960]

I. INTRODUCTION

Thixotropic and antithixotropic fluids, long studied by rheologists, have recently attracted wider interest within fluid dynamics as both their applications and the challenges they present have become better known. Thixotropic fluids are characterised by a gradual decrease of viscosity under increased shear and its gradual increase when shear is reduced; antithixotropic (rheopectic) fluids exhibit the opposite behaviour. Thixotropy is a property of many everyday fluids, including foods such as tomato sauce and some paints;[1] antithixotropy, though rarer, is observed in materials such as carbon black suspensions.[2]

Both thixotropy and antithixotropy arise because the fluid has an internal mesoscopic structure, which may consist of chains of molecules (such as polymers in crude oil) or other particles that can entangle or align in ways that affect the fluid's macroscopic properties. The dynamics of the mesostructure may be complicated and depend on factors such as temperature as well as on the macroscopic shear of the fluid. Frequently, thixotropic effects are associated with other rheological properties such as yield stress[3] or viscoelasticity.[4] In the present study we confine ourselves to ideal thixotropic fluids in the sense of Larson,[5] excluding viscoelastic effects, and we consider rheologies in which the state of the fluid structure is defined by a single scalar variable, the so-called structure parameter. Even within this category there are many rheological models to choose from to describe thixotropy and antithixotropy, reflecting the many contexts in which they arise.[1,3] This wide range of models means that there is a need for analytical studies that can distinguish generic behaviour from artefacts of a particular model.

A promising area for such studies is lubrication flow, in which the streamwise lengthscale is much greater than the transverse lengthscale and so the governing equations can be simplified asymptotically. Following its original development for Newtonian fluids,[6] lubrication theory has been extended formally to non-Newtonian fluids,[7–12] and recent work has explored various thixotropic effects in lubrication-type flows.[13–16] Recently, Pritchard, Wilson, and McArdle[17] (hereafter PWM) have derived a general theory for steady thixotropic and antithixotropic lubrication flows in a two-dimensional channel.

The present study develops PWM's approach in two important directions. We extend their analysis of steady flow to unsteady flow, in which the driving pressure gradients and thus the volume flux of fluid along the pipe may vary on a different time scale from the structure. Although loose analogies can be drawn between thixotropic effects in steady and in unsteady flow, we will show that these analogies can be misleading. Further, we consider axisymmetric flow in a slowly varying pipe of circular cross section. Such geometries have many industrial applications, including the transport of processed food, drilling muds, and crude oil.[13,18,19]

PWM presented results for the steady flow of thixotropic fluids in a widening channel. They found that thixotropy reduces the structure parameter throughout the channel, most strongly in the centre; meanwhile, it reduces the streamwise velocity near the walls but increases it in the centre of the channel. (See, e.g., Fig. 2 of PWM.) We will refer to this qualitative behaviour as the *thixotropic reference case* (TRC). PWM presented a physical interpretation of the TRC and suggested that it represents the generic effect of thixotropy or antithixotropy in an appropriate regime. We will discuss this interpretation below in the light of our new results and will present a refined version that elucidates the limits of such generic predictions.

In Sec. II we present and non-dimensionalise the governing equations, obtaining both an advective Deborah number $\mathcal{D}_a$, as obtained by PWM, and a new temporal Deborah number $\mathcal{D}_t$. We then perform an expansion in terms of the small aspect ratio δ of the flow. In Sec. III we consider the weakly advective and quickly adjusting regime in which $\mathcal{D}_a = \mathcal{O}(\delta)$ and $\mathcal{D}_t = \mathcal{O}(\delta)$, which allows us to study

[a] david.pritchard@strath.ac.uk

the advective and temporal effects of thixotropy in combination or in isolation. We obtain semi-analytical solutions for the streamwise and radial velocities and the structure parameter, from which we can obtain analytical or numerical solutions for specific rheological models. We illustrate these general results by considering first (Sec. IV A) the purely viscous Moore–Mewis–Wagner (MMW) model and then (Sec. IV B) the viscoplastic Houška model.

II. GEOMETRY AND GOVERNING EQUATIONS

A. Governing equations and boundary conditions

We consider the unsteady axisymmetric flow of an incompressible thixotropic or antithixotropic fluid along a cylindrical pipe of slowly varying radius, driven by a pressure gradient. A sketch of the problem is shown in Fig. 1, where $\hat{w}(\hat{r},\hat{z},\hat{t})$ and $\hat{u}(\hat{r},\hat{z},\hat{t})$ are the velocity components in the streamwise and radial directions, respectively, and $\lambda(\hat{r},\hat{z},\hat{t})$ is the structure parameter. (A caret denotes a dimensional quantity.) We take the typical streamwise lengthscale $\hat{L}$ of the flow to be much larger than the typical radial lengthscale $\hat{R}$, so the flow has the small aspect ratio $\hat{R}/\hat{L} = \delta \ll 1$.

The flow is governed by the mass conservation equation

$$\frac{1}{\hat{r}}\frac{\partial}{\partial \hat{r}}(\hat{r}\hat{u}) + \frac{\partial \hat{w}}{\partial \hat{z}} = 0, \tag{1}$$

and the Cauchy momentum equations

$$\frac{\partial \hat{p}}{\partial \hat{r}} = \frac{1}{\hat{r}}\frac{\partial}{\partial \hat{r}}(\hat{r}\hat{\tau}_{rr}) + \frac{\partial \hat{\tau}_{rz}}{\partial \hat{z}} \tag{2}$$

and

$$\frac{\partial \hat{p}}{\partial \hat{z}} = \frac{1}{\hat{r}}\frac{\partial}{\partial \hat{r}}(\hat{r}\hat{\tau}_{zr}) + \frac{\partial \hat{\tau}_{zz}}{\partial \hat{z}}. \tag{3}$$

Here $\hat{p}(\hat{z},\hat{t})$ is the pressure and $\hat{\tau}$ is the stress tensor, taken to be of generalised Newtonian form,

$$\hat{\tau}_{ij} = \hat{\eta}(\dot{\gamma},\lambda)\hat{e}_{ij}, \tag{4}$$

where $\hat{e}_{ij}$ denotes the strain-rate tensor and the apparent viscosity $\hat{\eta}$ depends on both the shear rate $\dot{\gamma} = \sqrt{\frac{1}{2}\hat{e}_{ij}\hat{e}_{ij}}$ and the structure parameter λ.

The structure of the fluid evolves according to an advection–kinetic equation, which describes the breakdown and build-up of the structure in a fluid element. This equation takes the general form

$$\frac{\mathrm{D}\lambda}{\mathrm{D}\hat{t}} = \hat{f}(\hat{\Gamma},\lambda), \tag{5}$$

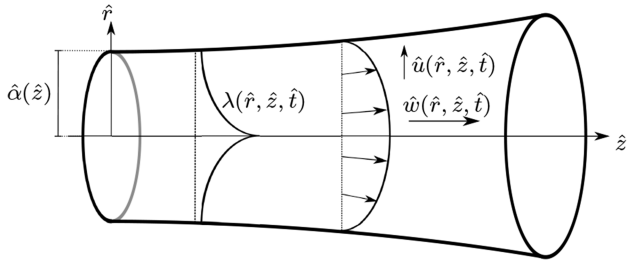

FIG. 1. Unsteady axisymmetric flow of a thixotropic or antithixotropic fluid along a cylindrical pipe of slowly varying radius $\hat{r} = \hat{\alpha}(\hat{z})$.

where $\mathrm{D}/\mathrm{D}\hat{t}$ denotes the material derivative, $\hat{f}(\hat{\Gamma},\lambda)$ describes the breakdown and buildup of the structure, and for convenience we define

$$\hat{\Gamma} = \dot{\gamma}^2 = 2\left(\frac{\partial \hat{u}}{\partial \hat{r}}\right)^2 + \left(\frac{\partial \hat{u}}{\partial \hat{z}} + \frac{\partial \hat{w}}{\partial \hat{r}}\right)^2 + 2\left(\frac{\partial \hat{w}}{\partial \hat{z}}\right)^2. \tag{6}$$

We assume that the usual no-slip boundary condition applies at the pipe wall, along with symmetry conditions at the centreline of the pipe, so that

$$\begin{aligned} \hat{u} = 0 = \hat{w} \text{ at } \hat{r} = \hat{\alpha}(\hat{z}),\\ \hat{\tau}_{rz} = 0 = \hat{u} \text{ at } \hat{r} = 0. \end{aligned} \tag{7}$$

Finally, since the fluid is incompressible, the streamwise volume flux is independent of $\hat{z}$,

$$2\pi \int_0^{\hat{\alpha}(\hat{z})} \hat{w}(\hat{r},\hat{z},\hat{t})\hat{r}\,\mathrm{d}\hat{r} = \hat{Q}(\hat{t}), \tag{8}$$

where $\hat{Q}(\hat{t})$ is specified as a global boundary condition.

B. Non-dimensionalisation

We non-dimensionalise and rescale the problem, defining dimensionless quantities via

$$\begin{aligned} &\hat{r} = \hat{R}r, \quad \hat{\alpha} = \hat{R}\alpha, \quad \hat{z} = \frac{\hat{R}z}{\delta}, \quad \hat{u} = \frac{\delta \hat{Q}_{\mathrm{ref}} u}{\hat{R}^2},\\ &\hat{w} = \frac{\hat{Q}_{\mathrm{ref}} w}{\hat{R}^2}, \quad \hat{\Gamma} = \frac{\hat{Q}_{\mathrm{ref}}^2 \Gamma}{\hat{R}^6}, \quad \hat{Q} = \hat{Q}_{\mathrm{ref}} Q,\\ &\hat{p} = \frac{\hat{\mu}_0 \hat{Q}_{\mathrm{ref}} p}{\delta \hat{R}^3}, \quad \hat{\eta} = \hat{\mu}_0 \eta, \quad \hat{t} = \hat{T}t, \quad \hat{f} = \hat{f}_0 f, \end{aligned} \tag{9}$$

where $\hat{Q}_{\mathrm{ref}}$ is the typical volume flux, $\hat{f}_0$ is the typical breakdown or build-up rate, $\hat{\mu}_0$ is the typical viscosity, and $\hat{T}$ is the typical time scale of the flow.

Using these dimensionless quantities, the mass conservation equation (1) becomes

$$\frac{1}{r}\frac{\partial}{\partial r}(ru) + \frac{\partial w}{\partial z} = 0, \tag{10}$$

and the Cauchy momentum equations (2) and (3), with constitutive law (4), become

$$\begin{aligned} \frac{\partial p}{\partial r} = {}& \delta^2\left[\frac{1}{r}\frac{\partial}{\partial r}\left(2r\eta\frac{\partial u}{\partial r}\right) + \frac{\partial}{\partial z}\left(\eta\frac{\partial w}{\partial r}\right)\right]\\ &+ \delta^4\frac{\partial}{\partial z}\left(\eta\frac{\partial u}{\partial z}\right), \end{aligned} \tag{11}$$

$$\begin{aligned} \frac{\partial p}{\partial z} = {}& \frac{1}{r}\frac{\partial}{\partial r}\left(r\eta\frac{\partial w}{\partial r}\right)\\ &+ \delta^2\left[\frac{1}{r}\frac{\partial}{\partial r}\left(r\eta\frac{\partial u}{\partial z}\right) + \frac{\partial}{\partial z}\left(2\eta\frac{\partial w}{\partial z}\right)\right]. \end{aligned} \tag{12}$$

The expression for Γ, given by (6), becomes

$$\Gamma = \left(\frac{\partial w}{\partial r}\right)^2 + \delta^2\left[2\left(\frac{\partial u}{\partial r}\right)^2 + 2\frac{\partial u}{\partial z}\frac{\partial w}{\partial r} + 2\left(\frac{\partial w}{\partial z}\right)^2\right] + \delta^4\left(\frac{\partial u}{\partial z}\right)^2. \tag{13}$$

After non-dimensionalisation, the boundary conditions (7) become

$$u = 0 = w \text{ at } r = \alpha(z),$$
$$\eta \frac{\partial w}{\partial r} = 0 = u \text{ at } r = 0, \tag{14}$$

and the flux condition (8) becomes

$$2\pi \int_0^{\alpha(z)} w(r,z,t) r \, \mathrm{d}r = Q(t). \tag{15}$$

Finally, the structure evolution equation (5) becomes

$$\mathcal{D}_\mathrm{t} \frac{\partial \lambda}{\partial t} + \mathcal{D}_\mathrm{a} \left(u \frac{\partial \lambda}{\partial r} + w \frac{\partial \lambda}{\partial z} \right) = f(\Gamma, \lambda), \tag{16}$$

where

$$\mathcal{D}_\mathrm{t} = \frac{1}{\hat{f}_0 \hat{T}} \quad \text{and} \quad \mathcal{D}_\mathrm{a} = \frac{\hat{Q}_\mathrm{ref} \delta}{\hat{f}_0 \hat{R}^3} \tag{17}$$

are the temporal and advective Deborah numbers, respectively. We note that $\mathcal{D}_\mathrm{a}$ can also be interpreted as the reciprocal of a "thixotropy number" as defined by Wachs *et al.*[13] or as a "thixoviscous number" as proposed by Ewoldt and McKinley,[20] but in order to compare advective and temporal effects directly, it is more informative to follow PWM by interpreting this parameter as a Deborah number.

C. General expansion scheme

We expand the dependent variables in powers of the aspect ratio δ,

$$(u, w, p, \lambda) = \sum_{i=0}^{\infty} \delta^i (u_i, w_i, p_i, \lambda_i). \tag{18}$$

From (11), the pressure depends on r only at $\mathcal{O}(\delta^2)$ and higher, so p_0 and p_1 are independent of r. We also expand Γ, $\eta(\Gamma, \lambda)$, and $f(\Gamma, \lambda)$,

$$\begin{aligned} \Gamma &= \Gamma_0 + \delta\Gamma_1 + \mathcal{O}(\delta^2), \\ \eta &= \eta_0 + \delta\eta_1 + \mathcal{O}(\delta^2), \\ f &= f_0 + \delta f_1 + \mathcal{O}(\delta^2), \end{aligned} \tag{19}$$

where

$$\begin{aligned} \Gamma_0 &= \left(\frac{\partial w_0}{\partial r} \right)^2, \quad \Gamma_1 = 2 \frac{\partial w_0}{\partial r} \frac{\partial w_1}{\partial r}, \\ \eta_0 &= \eta(\Gamma_0, \lambda_0), \quad \eta_1 = \eta_\Gamma \Gamma_1 + \eta_\lambda \lambda_1, \\ f_0 &= f(\Gamma_0, \lambda_0), \quad f_1 = f_\Gamma \Gamma_1 + f_\lambda \lambda_1, \end{aligned} \tag{20}$$

and where for convenience we have written

$$\begin{aligned} \eta_\Gamma &= \left. \frac{\partial \eta}{\partial \Gamma} \right|_{(\Gamma_0, \lambda_0)}, \quad \eta_\lambda = \left. \frac{\partial \eta}{\partial \lambda} \right|_{(\Gamma_0, \lambda_0)}, \\ f_\Gamma &= \left. \frac{\partial f}{\partial \Gamma} \right|_{(\Gamma_0, \lambda_0)}, \quad f_\lambda = \left. \frac{\partial f}{\partial \lambda} \right|_{(\Gamma_0, \lambda_0)}. \end{aligned} \tag{21}$$

Using (18)–(21), at $\mathcal{O}(1)$ Eqs. (10) and (12) yield

$$\frac{1}{r} \frac{\partial}{\partial r} (r u_0) + \frac{\partial w_0}{\partial z} = 0, \tag{22}$$

$$\frac{1}{r} \frac{\partial}{\partial r} \left(r \eta_0 \frac{\partial w_0}{\partial r} \right) = -G_0(z,t), \tag{23}$$

respectively, where $G_0(z,t) = -\partial p_0 / \partial z$. At $\mathcal{O}(1)$ the boundary conditions (14) yield

$$u_0 = 0 = w_0 \text{ at } r = \alpha(z),$$
$$\eta_0 \frac{\partial w_0}{\partial r} = 0 = u_0 \text{ at } r = 0, \tag{24}$$

and at $\mathcal{O}(1)$ the volume flux condition (15) yields

$$2\pi \int_0^{\alpha(z)} w_0(r,z,t) r \, \mathrm{d}r = Q(t). \tag{25}$$

Similarly, at $\mathcal{O}(\delta)$ Eqs. (10) and (12) yield

$$\frac{1}{r} \frac{\partial}{\partial r} (r u_1) + \frac{\partial w_1}{\partial z} = 0, \tag{26}$$

$$\frac{1}{r} \frac{\partial}{\partial r} \left[r \left(\eta_0 \frac{\partial w_1}{\partial r} + \left(2\eta_\Gamma \frac{\partial w_0}{\partial r} \frac{\partial w_1}{\partial r} + \eta_\lambda \lambda_1 \right) \frac{\partial w_0}{\partial r} \right) \right] = -G_1(z,t), \tag{27}$$

respectively, where $G_1(z,t) = -\partial p_1 / \partial z$. At $\mathcal{O}(\delta)$ the boundary conditions (14) yield

$$u_1 = 0 = w_1 \quad \text{at} \quad r = \alpha(z), \tag{28}$$

$$\eta_0 \frac{\partial w_1}{\partial r} + \left(2\eta_\Gamma \frac{\partial w_0}{\partial r} \frac{\partial w_1}{\partial r} + \eta_\lambda \lambda_1 \right) \frac{\partial w_0}{\partial r} = 0 \quad \text{and} \quad u_1 = 0 \quad \text{at} \quad r = 0, \tag{29}$$

and at $\mathcal{O}(\delta)$ the volume flux condition (15) yields

$$2\pi \int_0^{\alpha(z)} w_1(r,z,t) r \, \mathrm{d}r = 0. \tag{30}$$

The structure evolution equation (16) becomes

$$\begin{aligned} &\mathcal{D}_\mathrm{t} \left(\frac{\partial \lambda_0}{\partial t} + \delta \frac{\partial \lambda_1}{\partial t} \right) + \mathcal{D}_\mathrm{a} \left[u_0 \frac{\partial \lambda_0}{\partial r} + w_0 \frac{\partial \lambda_0}{\partial z} \right. \\ &\qquad \left. + \delta \left(u_1 \frac{\partial \lambda_0}{\partial r} + w_1 \frac{\partial \lambda_0}{\partial z} + u_0 \frac{\partial \lambda_1}{\partial r} + w_0 \frac{\partial \lambda_1}{\partial z} \right) \right] \\ &\qquad = f_0 + \delta \left(2 f_\Gamma \frac{\partial w_0}{\partial r} \frac{\partial w_1}{\partial r} + f_\lambda \lambda_1 \right). \end{aligned} \tag{31}$$

It is clear from (31) that the role of thixotropy depends on the relative magnitudes of the Deborah numbers $\mathcal{D}_\mathrm{t}$ and $\mathcal{D}_\mathrm{a}$ and the aspect ratio δ. PWM discussed the possible regimes in terms of $\mathcal{D}_\mathrm{a}$: these range from regimes in which the fluid structure adjusts so quickly to changes in the local shear rate that the fluid behaves to $\mathcal{O}(\delta)$ like a generalised Newtonian fluid, through to regimes in which the effects of breakdown and buildup enter at the same order as the $\mathcal{O}(\delta^2)$ geometrical corrections to classical lubrication theory. In the present study we focus on "quickly adjusting" regimes in which $\mathcal{D}_\mathrm{t} = \mathcal{O}(\delta)$ and "weakly advective" regimes in which $\mathcal{D}_\mathrm{a} = \mathcal{O}(\delta)$. In such regimes, thixotropic effects enter the equations at $\mathcal{O}(\delta)$, i.e., they are perturbations to the leading-order (generalised Newtonian) behaviour but enter at lower order than the $\mathcal{O}(\delta^2)$ geometrical corrections to classical lubrication theory.

III. GENERAL SOLUTIONS IN WEAKLY THIXOTROPIC REGIMES

We now specialise to the quickly adjusting and weakly advective regime, in which $\mathcal{D}_\mathrm{a} = \mathcal{O}(\delta)$ and $\mathcal{D}_\mathrm{t} = \mathcal{O}(\delta)$. We thus

define $\mathcal{D}_t = \delta\mathcal{D}_t^*$ and $\mathcal{D}_a = \delta\mathcal{D}_a^*$, where $\mathcal{D}_t^*$ and $\mathcal{D}_a^*$ are $\mathcal{O}(1)$ or smaller.

We consider the problem up to $\mathcal{O}(\delta)$, to which accuracy we can obtain two further regimes as limiting cases. The weakly advective and very quickly adjusting regime ($\mathcal{D}_a = \mathcal{O}(\delta)$ and $\mathcal{D}_t = \mathcal{O}(\delta^2)$) corresponds to steady flow, while the quickly adjusting and very weakly advective regime ($\mathcal{D}_t = \mathcal{O}(\delta)$ and $\mathcal{D}_a = \mathcal{O}(\delta^2)$) corresponds to spatially uniform flow. We will use this terminology below in order to simplify our discussion.

A. General form of the solution at $\mathcal{O}(1)$

At leading order, $\mathcal{O}(1)$, the flow is governed by the mass conservation equation (22) and the momentum equation (23), together with the structure evolution equation (31) which at leading order becomes simply

$$f_0 = 0. \tag{32}$$

These are to be solved subject to the leading-order boundary conditions (24) and the volume flux condition (25).

General semi-analytical solutions to the leading-order problem can be obtained following the approach of PWM; the advantage of this approach is that the derivatives required in the first-order solutions can be obtained as integrals and readily evaluated. For brevity we omit the details of the derivation here.

At leading order, the fluid has an implicitly defined generalised Newtonian rheology,

$$\tau(q) = \eta(q^2, \lambda_0)q \quad \text{subject to} \quad f(q^2, \lambda_0) = 0, \quad \text{where} \quad q = \frac{\partial w_0}{\partial r}. \tag{33}$$

For a given flux $Q(t)$, the pressure gradient G_0 is defined implicitly by the condition (25), which becomes

$$Q(t) = \frac{8\pi}{[G_0(z,t)]^3}\int_0^{q_w} q\tau^2(q)\tau'\,\mathrm{d}q, \tag{34}$$

where

$$q_w(z,t) = q(\alpha(z), z, t), \quad \text{so} \quad \tau(q_w) = -\frac{G_0(z,t)\alpha(z)}{2}. \tag{35}$$

The streamwise velocity is given by

$$w_0(r,z,t) = \frac{2}{G_0(z,t)}\int_{-G_0(z,t)r/2}^{-G_0(z,t)\alpha(z)/2} \tau^{-1}(\xi)\,\mathrm{d}\xi. \tag{36}$$

Finally, the radial velocity is given by

$$u_0(r,z,t) = \frac{r}{2G_0}\left(\frac{\partial G_0}{\partial z}w_0 + q_w\frac{\partial}{\partial z}[G_0\alpha]\right) + \frac{12}{G_0^4 r}\frac{\partial G_0}{\partial z}\int_0^q q\tau^2(q)\tau'(q)\,\mathrm{d}q. \tag{37}$$

B. General form of the solution at $\mathcal{O}(\delta)$

At first order, $\mathcal{O}(\delta)$, the perturbations satisfy the mass conservation equation (26), the momentum equation (27), and the $\mathcal{O}(\delta)$ structure evolution equation (31), namely,

$$\mathcal{D}_t^*\frac{\partial\lambda_0}{\partial t} + \mathcal{D}_a^*\left(u_0\frac{\partial\lambda_0}{\partial r} + w_0\frac{\partial\lambda_0}{\partial z}\right) = 2f_\Gamma\frac{\partial w_0}{\partial r}\frac{\partial w_1}{\partial r} + f_\lambda\lambda_1, \tag{38}$$

subject to the boundary conditions (28) and (29) and volume flux condition (30).

Using (38) to eliminate λ_1 from (27) yields

$$\frac{1}{r}\frac{\partial}{\partial r}\left[rA(r,z,t)\frac{\partial w_1}{\partial r} + rB(r,z,t)\right] = -G_1(z,t), \tag{39}$$

where

$$A = \eta_0 + 2\left(\eta_\Gamma - \eta_\lambda\frac{f_\Gamma}{f_\lambda}\right)\left(\frac{\partial w_0}{\partial r}\right)^2, \tag{40}$$

$$B = \frac{\eta_\lambda}{f_\lambda}\left[\mathcal{D}_t^*\frac{\partial\lambda_0}{\partial t} + \mathcal{D}_a^*\left(u_0\frac{\partial\lambda_0}{\partial r} + w_0\frac{\partial\lambda_0}{\partial z}\right)\right]\frac{\partial w_0}{\partial r}. \tag{41}$$

The term $A(r,z,t)$ represents the gradient of stress with respect to shear rate, while $B(r,z,t)$ represents the change to the stress due to the changing structure of the fluid. We will refer to $B(r,z,t)$ as the *thixotropic stress* term.

Integrating (39) with respect to r and applying the boundary condition (29) at $r = 0$ yields

$$\frac{\partial w_1}{\partial r} = -\left(\frac{1}{2}G_1(z,t)r + B(r,z,t)\right)\frac{1}{A(r,z,t)}, \tag{42}$$

from which a second integration with respect to r, applying the no-slip condition (28), yields

$$w_1(r,z,t) = \frac{G_1(z,t)}{2}\int_r^{\alpha(z)}\frac{r'}{A(r',z,t)}\,\mathrm{d}r' + \int_r^{\alpha(z)}\frac{B(r',z,t)}{A(r',z,t)}\,\mathrm{d}r'. \tag{43}$$

Finally, integrating (43) for a third time and applying the volume flux condition (30) yields

$$G_1(z,t) = -\frac{2\displaystyle\int_0^{\alpha(z)} r\int_r^{\alpha(z)}\frac{B(r',z,t)}{A(r',z,t)}\,\mathrm{d}r'\mathrm{d}r}{\displaystyle\int_0^{\alpha(z)} r\int_r^{\alpha(z)}\frac{r'}{A(r',z,t)}\,\mathrm{d}r'\mathrm{d}r}. \tag{44}$$

We note from (41) that $B(r,z,t)$ is the sum of an "advective" term proportional to $\mathcal{D}_a$ and a "temporal" term proportional to $\mathcal{D}_t$; from (44) and (43) we see that in fact all perturbation quantities can be decomposed in this manner. It is also evident that all advective terms must be proportional to α' and all temporal terms proportional to Q'. Consequently, in Sec. IV we need to consider only the cases of steady flow in a widening pipe ($\mathcal{D}_t^*Q' = 0$, $\mathcal{D}_a^*\alpha' > 0$) and of decelerating flow in a uniform pipe ($\mathcal{D}_a^*\alpha' = 0$, $\mathcal{D}_t^*Q' < 0$) in order to understand fully the behaviour of the fluid. Results for narrowing pipes and/or accelerating flows can be obtained by appropriate changes of sign or linear combinations of the "advective" and "temporal" perturbations, i.e., the perturbations in steady and in uniform flow, respectively.

IV. SOLUTIONS FOR SPECIFIC RHEOLOGIES

To gain insight into the range of possible thixotropic and antithixotropic behaviours, we investigate two specific rheologies. First, we consider the purely viscous Moore–Mewis–Wagner model, which allows us to explore both thixotropic

and antithixotropic effects. Second, we consider a regularised Houška model, which allows us to investigate the interaction between thixotropy and plasticity.

The thixotropic reference case (TRC) described in Sec. I guides our expectations about the form of the perturbations. We expect that in steady flow of a thixotropic fluid, the velocity perturbation w_1 will be positive near the centre and negative near the wall of the pipe, while the structure parameter perturbation λ_1 will be negative everywhere and largest in the centre of the pipe. Since antithixotropy is, loosely, the opposite of thixotropy, we may expect this picture to be reversed in steady flow of an antithixotropic fluid, so w_1 will be negative near the centre and positive near the wall, while λ_1 will be positive everywhere. We may also draw a loose analogy between decelerating flow and flow in a widening pipe, since the shear rate following a fluid element decreases in both cases. This leads us to expect that the perturbations in decelerating uniform flow will take the same forms as those in widening steady flow. However, as we will now show, not all of these expectations are fulfilled.

A. The MMW model

The MMW model employs a version of Moore's[21] constitutive law in which the viscosity is proportional to the structure parameter, so in dimensionless form

$$\eta = \lambda. \tag{45}$$

Meanwhile, λ satisfies Mewis and Wagner's[3] general structure evolution equation, in which

$$\hat{f}(\hat{\Gamma}, \lambda) = -\hat{k}_1 \hat{\Gamma}^{a/2} \lambda^b + \hat{k}_2 \hat{\Gamma}^{c/2} (1-\lambda)^d, \tag{46}$$

where the constants $\hat{k}_1$ and $\hat{k}_2$ specify the structural breakdown and build-up rates, and the exponents a, b, c, and d are non-negative.

We non-dimensionalise (46) following (9) with

$$\hat{f}_0 = \frac{\hat{k}_1 \hat{Q}_{\mathrm{ref}}^a}{\hat{R}^{3a}}, \tag{47}$$

to yield

$$f(\Gamma, \lambda) = -\Gamma^{a/2} \lambda^b + \kappa \Gamma^{c/2} (1-\lambda)^d, \quad \text{where} \quad \kappa = \frac{\hat{k}_2 \hat{Q}_{\mathrm{ref}}^{c-a}}{\hat{k}_1 \hat{R}^{3(c-a)}}. \tag{48}$$

The parameter κ represents the ratio of breakdown to build-up rates, and we assume that $\kappa = \mathcal{O}(1)$. In practice, breakdown rates may be rather larger than build-up rates so κ is numerically large; however, by taking it to be of order unity we obtain the dynamically richest problem, the greatest range of possible behaviours, and thus the most thorough test of our generic predictions.

In equilibrium, the structure parameter $\lambda = \lambda_{\mathrm{eq}}$ and the structure evolution rate is zero, from which we may obtain

$$\frac{\lambda_{\mathrm{eq}}^b}{(1-\lambda_{\mathrm{eq}})^d} = \kappa \Gamma^{(c-a)/2}. \tag{49}$$

Since the left-hand side is an increasing function of λ_{eq}, it is easy to see that when $c > a$, the structure increases with increasing shear rate (antithixotropy), whereas when $c < a$, the structure decreases with increasing shear rate (thixotropy).

When $d = 0$, the MMW model admits solutions in closed form, as in PWM; however, the usefulness of these solutions is undermined because they inherit the well-known centreline singularity of the power-law model.[11] We therefore consider only $d > 0$ here. For the MMW model with $d > 0$ we are unable to find analytical solutions in closed form for general d. We proceed instead using the general solutions for the leading-order problem, given in Sec. III A, and the general solutions for the first-order problem, given in Sec. III B, though we must evaluate the integrals in these solutions numerically; the results shown here were generated using the computer algebra package Maple.[22]

Figure 2 illustrates the leading-order profiles of the streamwise velocity and structure parameter for typical thixotropic and antithixotropic cases. They have the familiar forms associated with shear-thinning and shear-thickening pipe flow: the thixotropic fluid is most structured at the centreline of the pipe, and so the velocity profile is "blunt" near the centreline; conversely, the antithixotropic fluid is least structured at the centreline, and so the velocity profile is "sharper."

Figure 3 illustrates the corresponding perturbations to the velocity and the structure parameter, both for steady flow in a widening pipe ($\mathcal{D}_a \alpha' = 1$, $\mathcal{D}_t Q' = 0$) and for decelerating flow in a uniform pipe ($\mathcal{D}_a \alpha' = 0$, $\mathcal{D}_t Q' = -1$). For a thixotropic fluid [Figs. 3(a) and 3(c)], the forms of the perturbations agree with the thixotropic reference case of PWM: the velocity perturbation is positive near the centre of the pipe and negative

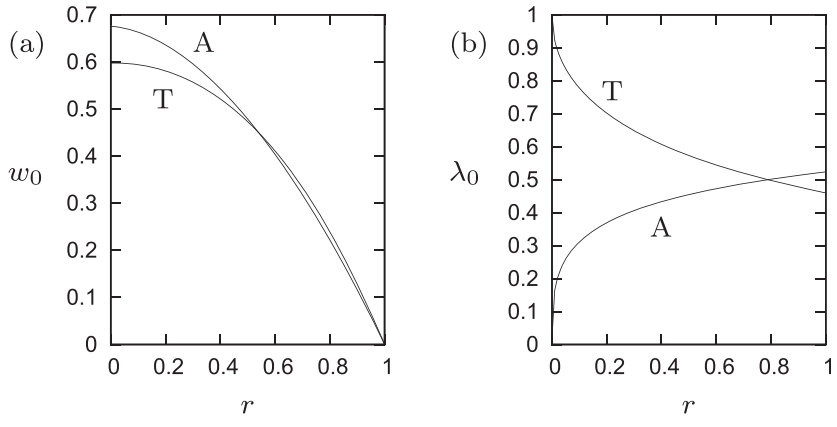

FIG. 2. MMW model: leading-order solutions for (a) streamwise velocity w_0 and (b) structure parameter λ_0. Thixotropic fluid (T): $a = 1$, $c = 0.5$. Antithixotropic fluid (A): $a = 0.5$, $c = 1$. Common parameter values: $b = 1$, $d = 1$, and $\kappa = 1$.

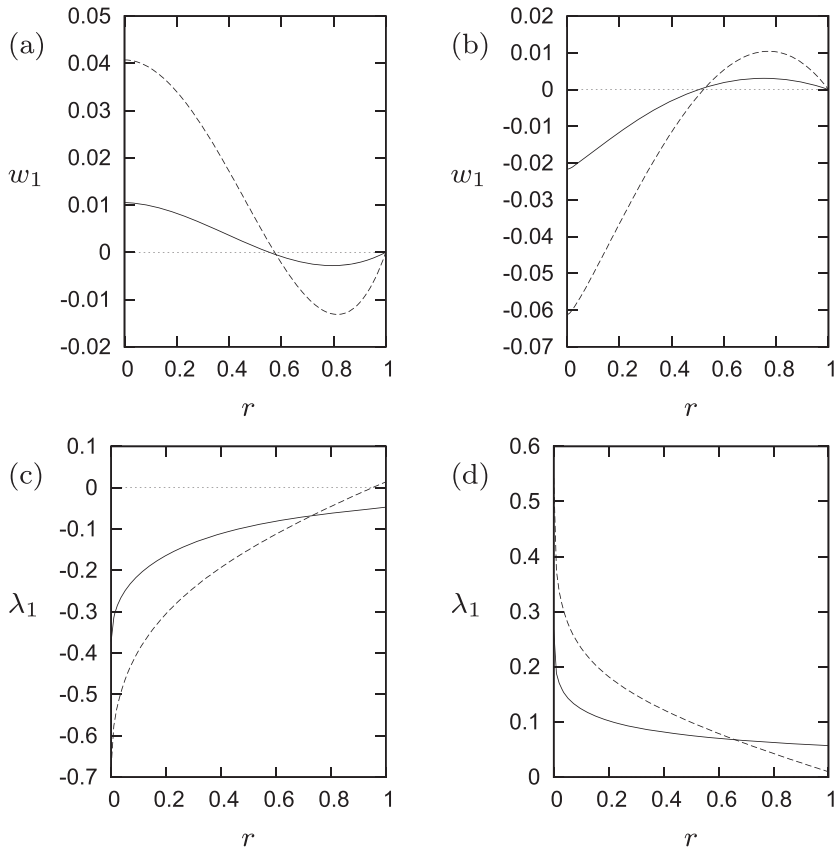

FIG. 3. MMW model: perturbations to [(a) and (b)] streamwise velocity w_1 and [(c) and (d)] structure parameter λ_1, for [(a) and (c)] thixotropic fluid with $a=1$, $c=0.5$; [(b) and (d)] antithixotropic fluid with $a=0.5$, $c=1$. Solid lines denote uniform flow ($\mathcal{D}_a\alpha'=0$, $\mathcal{D}_t\mathcal{Q}'=-1$); dashed lines denote steady flow ($\mathcal{D}_a\alpha'=1$, $\mathcal{D}_t\mathcal{Q}'=0$). Common parameter values: $b=1$, $d=1$, and $\kappa=1$.

nearer the wall, while the structure perturbation is generally negative, and largest at the centre (although it becomes positive at the wall in steady flow). The perturbations in steady flow are generally larger than those in uniform flow. As one might expect, the antithixotropic fluid behaves conversely: the velocity perturbation is negative near the centre of the pipe and positive nearer the wall, while the structure perturbation is generally positive, and largest at the centre [Figs. 3(b) and 3(d)]. (We also note that the perturbations in steady and in uniform flow do not have the same cross-pipe structure, meaning that perfect cancellation of advective and temporal effects in, for example, accelerating flow in a widening pipe, is not possible.)

The cases plotted in Fig. 3 do not, however, represent the full spectrum of possible behaviour of the MMW model. Figure 4 illustrates another possibility, which can occur when the fluid is sufficiently strongly thixotropic or antithixotropic. The velocity gradient $\partial w_1/\partial r$ now changes sign again near the centre of the pipe [Fig. 4(a)], so the velocity perturbation has a local minimum rather than a local maximum at $r=0$, and its maximum value is thus somewhat smaller than in less strongly thixotropic cases. In this regime, the structure perturbation λ_1 drops to zero at the centre [Fig. 4(b)]. An asymptotic analysis of the behaviour of the perturbations near the centreline shows that this behaviour occurs when either $d<1$ and $a>c/(1-d)$ or $b<1$ and $c>a(1-b)$; we omit the details here for brevity.

The behaviour illustrated in Fig. 4 is a minor deviation from the TRC, and in practice it is only visible for rather extreme values of the exponents in (48); it is also much more conspicuous in uniform than in steady flow. Nevertheless, it

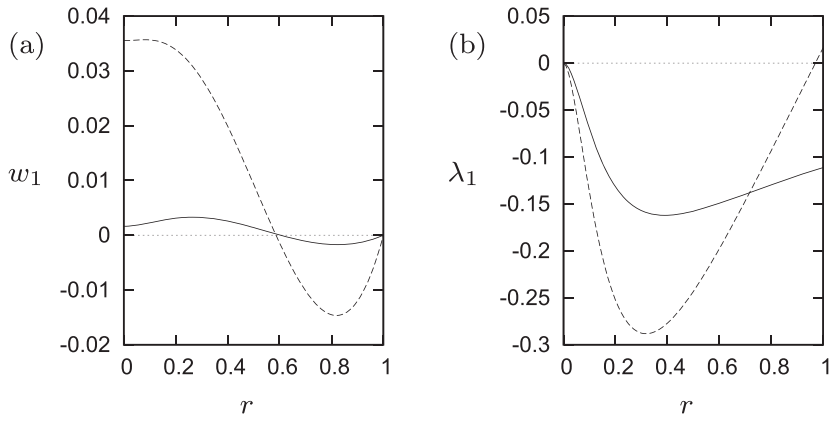

FIG. 4. MMW model: perturbations to (a) streamwise velocity w_1 and (b) structure parameter λ_1, for a strongly thixotropic fluid with $a=0.75$, $b=0.5$, $c=0.62$, $d=0.1$, and $\kappa=1$. Solid lines denote uniform flow ($\mathcal{D}_a\alpha'=0$, $\mathcal{D}_t\mathcal{Q}'=-1$); dashed lines denote steady flow ($\mathcal{D}_a\alpha'=1$, $\mathcal{D}_t\mathcal{Q}'=0$).

is interesting because of its paradoxical nature: stronger deviations from Newtonian rheology are associated with smaller perturbations to generalised Newtonian flow. It also suggests that PWM's physical interpretation of the TRC is incomplete; we will return to this following our investigation of the Houška model.

B. The regularised Houška model

In many contexts,[3,5,23] thixotropy occurs in conjunction with a yield stress. The simplest rheological model that combines these phenomena is the Houška model,[24] which combines a Herschel–Bulkley constitutive law[25] with a structure parameter that obeys a special case of Mewis and Wagner's structure evolution equation.[3] In order to apply the semi-analytical approach described in Sec. III, we regularise this model following the approach of Papanastasiou.[26]

In dimensional terms, the regularised Houška rheology is defined by

$$\hat{\eta}(\dot{\gamma},\lambda) = \frac{\hat{\tau}_y(\lambda)(1-\mathrm{e}^{-\hat{k}\dot{\gamma}})}{\dot{\gamma}} + \hat{\eta}_H(\lambda)\dot{\gamma}^{n-1}, \tag{50}$$

where the regularisation parameter $\hat{k}$ is large relative to the reciprocal of typical shear rates in the flow. (The effect of the regularisation can be seen in Figs. 5 and 6, in the form of a slight rounding of the edges of the pseudo-plug.) We will take $n=1$ throughout. The yield stress $\hat{\tau}_y(\lambda)$ and the viscosity $\hat{\eta}_H(\lambda)$ are linear functions of λ, given by

$$\hat{\tau}_y(\lambda) = \hat{\tau}_{y0} + \lambda\hat{\tau}_{y1} \quad \text{and} \quad \hat{\eta}_H(\lambda) = \hat{\eta}_{H0} + \lambda\hat{\eta}_{H1}. \tag{51}$$

The structure evolution rate is given by setting $a=1$, $b=1$, $c=0$, and $d=1$ in (46), to obtain

$$\hat{f}(\hat{\Gamma},\lambda) = -\hat{k}_1\hat{\Gamma}^{1/2}\lambda + \hat{k}_2(1-\lambda). \tag{52}$$

We non-dimensionalise this model using (9) and (47) together with $\hat{\mu}_0 = \hat{\eta}_{H0}$, obtaining the dimensionless rheological parameters

$$\eta_{H1} = \frac{\hat{\eta}_{H1}}{\hat{\eta}_{H0}}, \quad \tau_{y0} = \frac{\hat{Q}_{ref}^2}{\hat{R}^6}\frac{\hat{\tau}_{y0}}{\hat{\eta}_{H0}}, \quad \tau_{y1} = \frac{\hat{Q}_{ref}^2}{\hat{R}^6}\frac{\hat{\tau}_{y1}}{\hat{\eta}_{H0}}, \quad k = \frac{\hat{Q}_{ref}^2\hat{k}}{\hat{R}^6}. \tag{53}$$

Figure 5 illustrates typical profiles of the unperturbed flow and the perturbations. The most conspicuous feature of the unperturbed flow [Figs. 5(a) and 5(b)] is the pseudo-plug in the centre of the pipe, within which the fluid is fully structured, $\lambda_0 = 1$, and the streamwise velocity is constant. The velocity perturbation [Fig. 5(c)] is similar to that for the purely viscous fluid considered in the thixotropic reference case, with reduced velocity next to the wall and increased velocity near the centre, particularly in the pseudo-plug region. The perturbation to the structure parameter [Fig. 5(d)] takes a different form: although as expected it is negative across most of the width of the pipe, it peaks at the edges of the pseudo-plug and is zero within it. This is due to the lack of shear in the pseudo-plug, which means that the structure there cannot evolve. Likewise, within the pseudo-plug the velocity perturbation is constant.

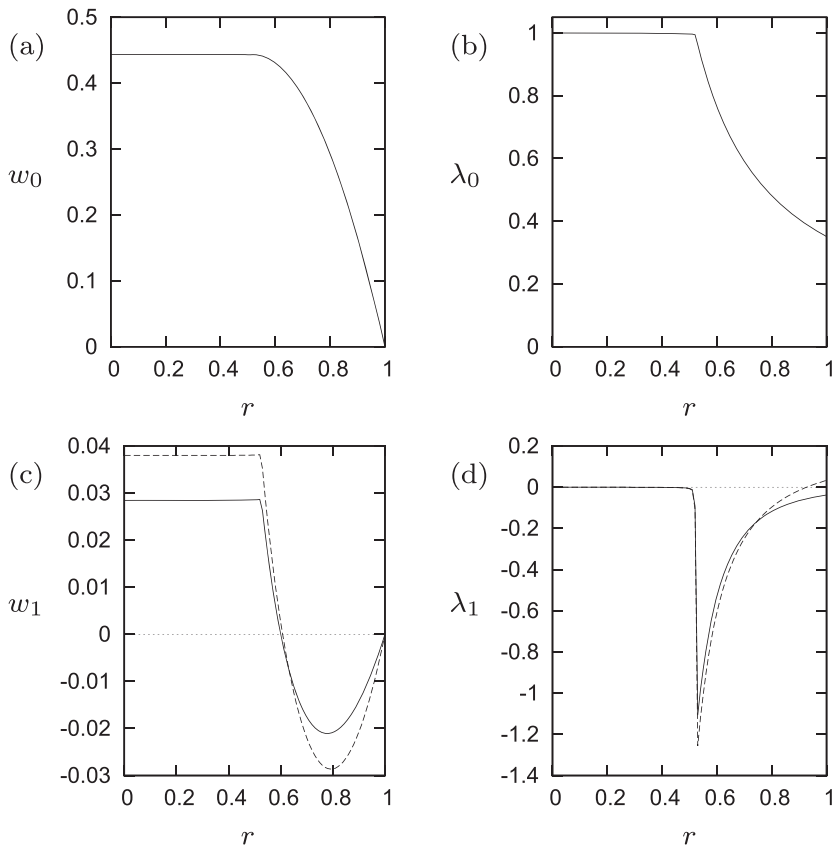

FIG. 5. Houška model: leading-order solutions for (a) streamwise velocity w_0 and (b) structure parameter λ_0, and perturbations to (c) velocity w_1 and (d) structure parameter λ_1. Solid lines denote uniform flow ($\mathcal{D}_a\alpha' = 0$, $\mathcal{D}_t Q' = -1$); dashed lines denote steady flow ($\mathcal{D}_a\alpha' = 1$, $\mathcal{D}_t Q' = 0$). Common parameter values: $\tau_{y0} = 1$, $\tau_{y1} = 1$, $\eta_{H1} = 1$, and $k = 1000$.

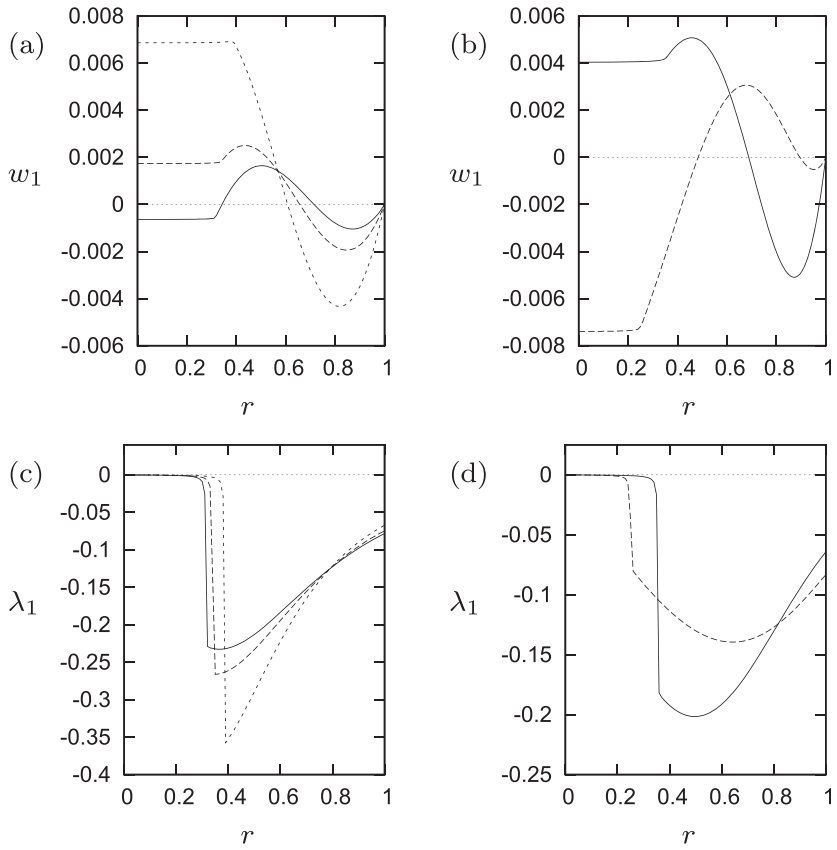

FIG. 6. Houška model: perturbations to [(a) and (b)] streamwise velocity w_1 and [(c) and (d)] structure parameter λ_1, for [(a) and (c)] $\eta_{H1} = 1$, with $\tau_{y1} = 0$ (solid), $\tau_{y1} = 0.1$ (dashed), and $\tau_{y1} = 0.3$ (light dashed); for [(b) and (d)] $\tau_{y1} = 1$, with $\eta_{H1} = 4$ (solid) and $\eta_{H1} = 8$ (dashed). All results are for uniform flow ($\mathcal{D}_a\alpha' = 0$, $\mathcal{D}_t\mathcal{Q}' = -1$). Common parameter values: $\tau_{y0} = 1$ and $k = 1000$.

This picture, however, is not universal, as Fig. 6 illustrates. In Figs. 6(a) and 6(c) we see the effect of reducing the parameter τ_{y1}, which controls the variation of the yield stress with λ. As τ_{y1} is reduced, the yield stress decreases and so the pseudo-plug becomes slightly narrower. A more conspicuous feature, however, is that the velocity perturbation w_1 is reduced within the pseudo-plug, eventually becoming negative so the effect of thixotropy on the flow is significantly different from the TRC: the velocity is now increased just outwith the pseudo-plug but decreased both within the pseudo-plug and near to the wall. A similar effect can be seen in Figs. 6(b) and 6(d) as the parameter η_{H1}, which controls the variation of the viscosity with λ, is increased.

C. Mechanisms controlling the velocity perturbation

To explain the behaviour in Figs. 4 and 6, we must investigate the factors controlling the velocity perturbation gradient $\partial w_1/\partial r$. From (42), and noting from (40) that $A(r, z, t) \geq 0$, this gradient is controlled by the interaction between two terms: a term $\frac{1}{2}G_1(z, t)r$ that represents the effect of the first-order pressure gradient that imposes the flux condition (30); and the thixotropic stress term $B(r, z, t)$, given by (41), which represents the direct effect of thixotropy or antithixotropy. It is clear from (42) that the sign of $\partial w_1/\partial r$ depends on which of these terms is larger. Figure 7 illustrates the balance of these terms in cases in which the form of the perturbations accords with expectations based on the TRC [Figs. 7(a) and 7(b)] and in cases in which it does not [Figs. 7(c) and 7(d)].

The thixotropic stress term B describes the effect of the evolving structure on the velocity gradient. It is proportional to the product of the Lagrangian derivative $\mathrm{D}\lambda_0/\mathrm{D}t$ and the local leading-order shear rate $\partial w_0/\partial r$. Since the shear rate vanishes at the centreline, $B = 0$ at $r = 0$ both in steady and in uniform flow. However, different boundary conditions control the value of B at the wall.

In steady flow, B is proportional to the advective derivative $\mathbf{u}_0 \cdot \nabla\lambda_0$, which vanishes at the wall due to the no-slip condition; thus, in steady flow, $B = 0$ at the wall as well as the centreline and is constrained to take the form in Figs. 7(a) and 7(c). This means that $\partial w_1/\partial r$ is inevitably negative at the wall and so w_1 is inevitably positive near the wall; the consequence is that velocity perturbations in steady flow can deviate only fairly subtly, near the centre of the pipe, from the generic behaviour suggested by the TRC.

In uniform flow, in contrast, B is proportional to the time derivative $\partial\lambda_0/\partial t$, which does not in general vanish at the wall. Figures 7(b) and 7(d) show that both $|B|$ and $|\frac{1}{2}G_1 r|$ increase from the centre of the pipe to the wall, and the balance between these two terms is much finer than in steady flow. Consequently, a slight change in the concavity of B can change the regions in which $\partial w_1/\partial r$ is positive and negative, leading to more complicated forms for w_1 than predicted by the TRC. In addition, because B is closer to $-\frac{1}{2}G_1 r$ in uniform than in steady flow, $\partial w_1/\partial r$ is generally smaller in uniform flow. This explains why $|w_1|$ in uniform flow is generally smaller than in steady flow (compare the dashed and solid lines in Fig. 3).

We can also explain the form of the velocity perturbations in the Houška model, and the reversal in sign of w_1 when η_{H1} is large or τ_{y1} is small. Figure 8 illustrates the balance between the thixotropic stress term and the pressure gradient term for the cases plotted in Figs. 6(b) and 6(d). Because the

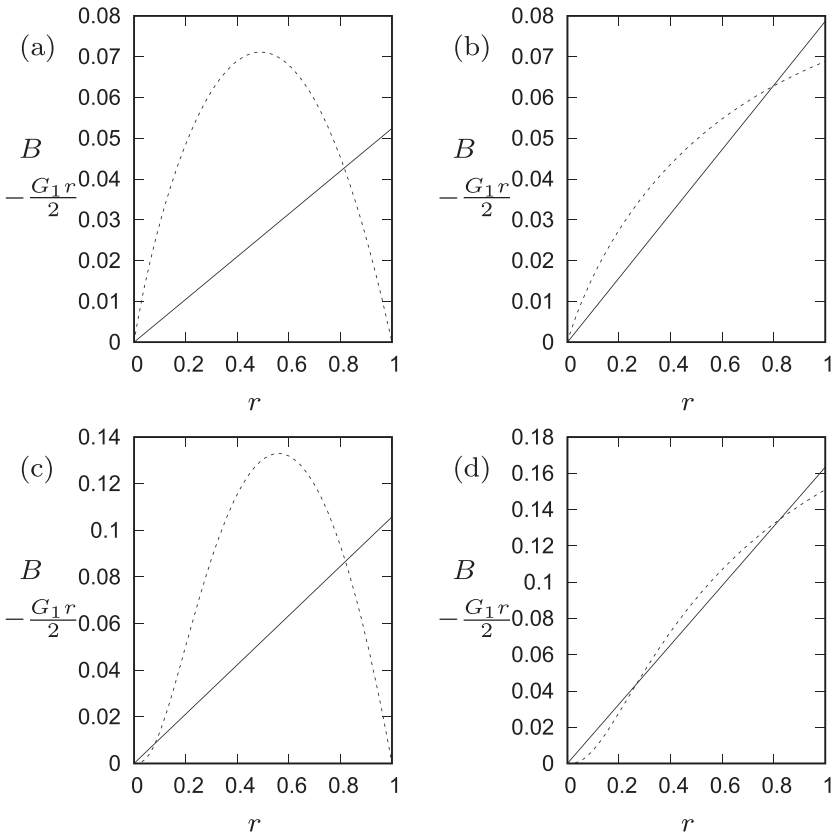

FIG. 7. MMW model: thixotropic stress term B (dashed) and pressure gradient term $-\frac{1}{2}G_1 r$ (solid), in [(a) and (c)] steady and [(b) and (d)] uniform flow, for [(a) and (b)] a thixotropic fluid with $a=1$, $b=1$, $c=0.5$, $d=1$, and $\kappa=1$; [(c) and (d)] a strongly thixotropic fluid with $a=0.75$, $b=0.5$, $c=0.62$, $d=0.1$, and $\kappa=1$.

thixotropic stress term is zero within the pseudo-plug, there are in general two intersections between B and $-\frac{1}{2}G_1 r$, and thus two turning points of w_1. As τ_{y1} decreases or η_{H1} increases, the viscous stresses become larger relative to the yield stress. The consequence is that the pseudo-plug becomes narrower for a given flux; consequently, the balance between B and $-\frac{1}{2}G_1 r$ becomes finer [Fig. 8(b)], and the turning points of w_1 move closer together. As a consequence, the positive region of w_1 becomes smaller, allowing w_1 to reverse within and just outwith the pseudo-plug.

D. Beyond the thixotropic reference case

With the results of Sec. IV C in mind, we can refine the apparently generic explanation of the TRC given by PWM. We recall that, for convenience, we consider widening pipes ($\alpha' > 0$) and decelerating flows ($Q' < 0$). We expect flow in a widening pipe and a decelerating flow to be loosely equivalent, and we also expect antithixotropic fluids to behave in the opposite way from thixotropic fluids. As we have seen, the analogies between widening pipes and decelerating flows, and between thixotropy and antithixotropy, provide useful heuristics but fail to capture all the behaviour of the perturbations.

The steady flow of a thixotropic fluid in a widening channel provides the TRC, in which w_1 is positive at the centre of the channel and negative at the wall, and λ_1 is negative across the width of the channel and largest at the centre. To explain the behaviour of the TRC, PWM reason that (a) the advection of broken-down fluid from upstream is strongest at the centre of the channel, so this is where λ, and therefore the viscosity, is most reduced relative to λ_{eq}; (b) fluid with a low viscosity is easiest to shear, so flows faster ($w_1 > 0$) near the centre of the

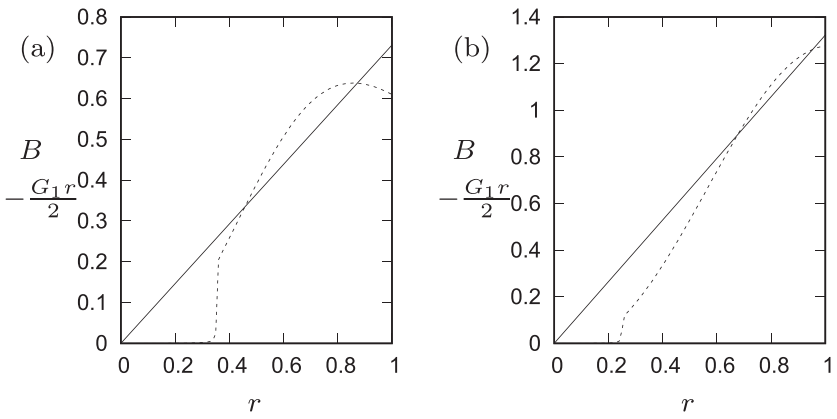

FIG. 8. Houška model: thixotropic stress term B (dashed) and pressure gradient term $-\frac{1}{2}G_1 r$ (solid), in uniform flow, for a thixotropic fluid with $\tau_{y0}=1$, $\tau_{y1}=1$, $k=1000$, and (a) $\eta_{H1}=4$; (b) $\eta_{H1}=8$.

channel; (c) as flux must be conserved, the increase in w near the centre must be offset by a decrease ($w_1 < 0$) near the wall. Although this explanation appears sufficient for the TRC, it is incomplete even for steady flow and, as we have seen, does not capture the dynamics of unsteady flow.

We are now in a position to refine PWM's explanation of the TRC in the following ways. (a) Although the advection of structure is strongest at the centre of the pipe, the temporal evolution of the structure may be fastest at the centre of the pipe or at the wall. (b) The advective component of the thixotropic stress term is zero at the centre of the pipe and at the wall, but the temporal component of the thixotropic stress term is weakest at the centre and strongest at the wall. (c) The pressure gradient G_1, which maintains the prescribed flux, affects the shear rate most strongly at the wall and most weakly at the centre. The advective component of the thixotropic stress term is always weaker at the wall than the pressure gradient term, which gives the characteristic shape of w_1 in the TRC, and this behaviour appears to be generic except very close to the centreline. In contrast, the temporal component of the thixotropic stress term may be larger or smaller than the pressure gradient term anywhere across the pipe, so we cannot predict the shape of the profile of w_1 in general.

In summary, although PWM's interpretation of the TRC is a useful heuristic for the advective effect of thixotropy, it cannot predict some of the finer details of where thixotropy-enhanced shear occurs, and does not capture the effect of antithixotropy in unsteady flow, which is more sensitive to the precise choice of rheology. This sensitivity suggests strongly that no entirely general predictions can be made of how antithixotropy affects the velocity profile in unsteady lubrication flow. In turn, this calls into question how generally it is possible to develop "reduced" models such as those proposed by Livescu *et al.*[14]

V. CONCLUSIONS

This study has extended the perturbation approach to weakly thixotropic lubrication flow developed by Pritchard, Wilson, and McArdle[17] (PWM) to unsteady pipe flows. Such flows are characterised by two Deborah numbers, one representing advective thixotropic effects and one representing temporal thixotropic effects; we have explored the "weakly advective" and "slowly adjusting" regimes in which these Deborah numbers are comparable with the small aspect ratio δ of the flow, and analytical or semi-analytical solutions may then be developed up to $\mathcal{O}(\delta)$. In the course of exploring these solutions, we have identified several deviations from the thixotropic reference case (TRC) that was presented as generic by PWM,[17] and this has allowed us to refine our understanding of the mechanisms that control the thixotropic or antithixotropic response.

We recall that in the TRC in a widening channel the streamwise velocity perturbation is positive near the centre of the pipe and negative near the wall, while the structure parameter perturbation is negative and largest at the centre of the pipe.[17] From the TRC we can predict the qualitative behaviour of an antithixotropic fluid or flow in a narrowing channel by an appropriate change of sign. A natural analogy may also be drawn between steady flow in a widening pipe and uniform flow with a decreasing volume flux, since in each case any given fluid element is decelerating. However, our results demonstrate that this analogy can be misleading.

Our exploration of the Moore–Mewis–Wagner model indicated that although in many cases its behaviour accords with the TRC, if the fluid is sufficiently strongly thixotropic or antithixotropic then deviations occur (Fig. 4): the velocity perturbation acquires additional turning points, and the structure parameter perturbation is no longer largest at the centre of the pipe. In a regularised viscoplastic Houška model, still more significant qualitative deviations from the TRC occur (Fig. 6). Notably, when the variation of the yield stress with the structure parameter is sufficiently weak or the variation of the viscosity with the yield stress is sufficiently strong, the velocity perturbation may peak at the edges of the pseudo-plug and then reverse within the plug, so thixotropy leads to slower flow in the centre of the channel.

The mechanism behind these changes involves the competition between the pressure gradient and a thixotropic stress term proportional to the Lagrangian derivative of the structure, considered as a function of position across the pipe. Crucially, the Lagrangian derivative takes rather different forms in steady and in uniform flow. Consequently, the analogy between flow in a widening pipe and flow with a decreasing flux is not complete; in unsteady uniform flow the balance between the pressure gradient and thixotropic stress terms is rather finer and so the perturbations are more prone to deviate from the TRC.

The underlying challenge in the mathematical modelling of thixotropic flow is to distinguish between phenomena that are generic and those that are artefacts of particular rheological models. A thorough understanding of this distinction is necessary in order to develop reliable means of constructing reduced-order flow models[14,16,17] as well as to extract physical insight from the findings of particular studies. The subtle nature of slowly varying thixotropic and antithixotropic flow revealed by the present perturbation approach indicates the scale of this challenge, since it must be expected that more complicated flow problems will prove still more resistant to general analysis. Nevertheless, this work provides a basis for further systematic studies of related flows, as well as an overview of possible dynamical regimes that may serve to guide future investigations in this area.

ACKNOWLEDGMENTS

A.I.C. is supported by a Doctoral Training Award (No. EP/L505080/1) funded by the United Kingdom Engineering and Physical Sciences Research Council (EPSRC). S.K.W. was partially supported by the Leverhulme Trust via Research Fellowship No. RF-2013-355. All data are provided in full in the results sections of this paper. We are grateful to two anonymous reviewers for their constructive comments on an earlier version of this work.

[1] H. A. Barnes, "Thixotropy—A review," J. Non-Newtonian Fluid Mech. **70**, 1–33 (1997).
[2] G. Ovarlez, L. Tocquer, F. Bertrand, and P. Coussot, "Rheopexy and tunable yield stress of carbon black suspensions," Soft Matter **9**, 5540–5549 (2013).

[3]J. Mewis and N. J. Wagner, "Thixotropy," Adv. Colloid Interface Sci. **147–148**, 214–227 (2009).
[4]M. Renardy and Y. Renardy, "Thixotropy in yield stress fluids as a limit of viscoelasticity," IMA J. Appl. Math. **81**, 522–537 (2016).
[5]R. G. Larson, "Constitutive equations for thixotropic fluids," J. Rheol. **59**, 595–611 (2015).
[6]O. Reynolds, "On the theory of lubrication and its application to Mr. Beauchamp Tower's experiments, including an experimental determination of the viscosity of olive oil," Philos. Trans. R. Soc. London **177**, 157–234 (1886).
[7]R. I. Tanner, *Engineering Rheology* (Oxford University Press, 1985).
[8]V. A. Gorodtsov, "Spreading of a film of nonlinearly viscous liquid over a horizontal smooth solid surface," J. Eng. Phys. **57**, 879–884 (1989). [Inzh.-Fiz. Zh. **57**(2), 203–209 (1989)].
[9]N. J. Balmforth and R. V. Craster, "A consistent thin-layer theory for Bingham plastics," J. Non-Newtonian Fluid Mech. **84**, 65–81 (1999).
[10]I. A. Frigaard and D. P. Ryan, "Flow of a visco-plastic fluid in a channel of slowly varying width," J. Non-Newtonian Fluid Mech. **123**, 67–83 (2004).
[11]T. G. Myers, "Application of non-Newtonian models to thin film flow," Phys. Rev. E **72** 066302 (2005).
[12]D. Pritchard, B. R. Duffy, and S. K. Wilson, "Shallow flows of generalised Newtonian fluids on an inclined plane," J. Eng. Math. **94**, 115–133 (2015).
[13]A. Wachs, G. Vinay, and I. Frigaard, "A 1.5D numerical model for the start up of weakly compressible flow of a viscoplastic and thixotropic fluid in pipelines," J. Non-Newtonian Fluid Mech. **159**, 81–94 (2009).
[14]S. Livescu, R. V. Roy, and L. W. Schwartz, "Leveling of thixotropic liquids," J. Non-Newtonian Fluid Mech. **166**, 395–403 (2011).
[15]D. R. Hewitt and N. J. Balmforth, "Thixotropic gravity currents," J. Fluid Mech. **727**, 56–82 (2013).
[16]A. S. Uppal, R. V. Craster, and O. K. Matar, "Dynamics of spreading thixotropic droplets," J. Non-Newtonian Fluid Mech. **240**, 1–14 (2017).
[17]D. Pritchard, S. K. Wilson, and C. R. McArdle, "Flow of a thixotropic or antithixotropic fluid in a slowly varying channel: The weakly advective regime," J. Non-Newtonian Fluid Mech. **238**, 140–157 (2016).
[18]A. Ahmadpour, K. Sadeghy, and S.-R. Maddah-Sadatieh, "The effect of a variable plastic viscosity on the restart problem of pipelines filled with gelled waxy crude oils," J. Non-Newtonian Fluid Mech. **205**, 16–27 (2014).
[19]S. Livescu, "Mathematical modeling of thixotropic drilling mud and crude oil flow in wells and pipelines—A review," J. Pet. Sci. Eng. **98–99**, 174–184 (2012).
[20]R. H. Ewoldt and G. H. McKinley, "Mapping thixo-elasto-visco-plastic behavior," Rheol. Acta **56**, 195–210 (2017).
[21]F. Moore, "The rheology of ceramic slips and bodies," Trans. Br. Ceram. Soc. **58**, 470–494 (1959).
[22]Maple, Maplesoft, a division of Waterloo Maple Inc., Waterloo, Ontario, 2016.
[23]M. M. Denn and D. Bonn, "Issues in the flow of yield-stress liquids," Rheol. Acta **50**, 307–315 (2011).
[24]M. Houška, "Inženýrské aspekty reologie tixotropních kapalin [Engineering aspects of the rheology of thixotropic fluids]," Ph.D. thesis, České vysoké učení technické v Praze [Czech Technical University in Prague], 1980.
[25]W. H. Herschel and R. Bulkley, "Konsistenzmessungen von Gummi-Benzollösungen," Kolloid-Z. **39**, 291–300 (1926).
[26]T. C. Papanastasiou, "Flows of materials with yield," J. Rheol. **31**, 385–404 (1987).